

# Quantitative proteomic dissection of a native 14-3-3 $\epsilon$ interacting protein complex associated with hepatocellular carcinoma

Chen Bai · Siwei Tang · Chen Bai · Xian Chen

Received: 26 October 2013 / Accepted: 11 December 2013 / Published online: 21 December 2013  
© Springer-Verlag Wien 2013

**Abstract** The 14-3-3 proteins regulate diverse biological processes that are implicated in cancer development, and seven 14-3-3 isoforms were identified with isoform-specific roles in different human tumors. In our previous work, we dissected the interactome of 14-3-3 $\epsilon$  formed during the DNA damage response in a hepatocellular carcinoma (HCC) cell using an AACT/SILAC-based quantitative proteomic approach. In this study, we used a similar proteomic approach to profile/identify the 14-3-3 $\epsilon$  interactome formed in native HCC cells. Functional categorization and data-dependent network analysis of the native HCC-specific 14-3-3 $\epsilon$  interactome revealed that 14-3-3 $\epsilon$  is involved in the regulation of multiple biological processes (BPs)/pathways, including cell cycle control, apoptosis, signal transduction, transport, cell adhesion, carbohydrate metabolism, and nucleic acid metabolism. Biological

validation further supports that 14-3-3 $\epsilon$ , via association with multiple BP/pathway-specific proteins, coordinates the regulation of proliferation, survival, and metastasis of HCC. The findings in this study, together with those of our previous study, provide an extensive profile of the 14-3-3 $\epsilon$  interaction network in HCC cells, which should be valuable for understanding the pathology of HCC and HCC therapy.

**Keywords** Hepatocellular carcinoma (HCC) · 14-3-3 $\epsilon$  · AACT/SILAC · LC–MS/MS

## Abbreviations

LC–MS/MS	Liquid chromatography coupled to tandem mass spectrometry
AACT	Amino acid-coded mass tagging
SILAC	Stable isotope labeling with amino acids in cell culture
Leu	Leucine
Leu-d <sub>3</sub>	Deuterium-labeled leucine (5,5,5-d <sub>3</sub> )

C. Bai and S. Tang contributed equally to this work.

**Electronic supplementary material** The online version of this article (doi:10.1007/s00726-013-1644-4) contains supplementary material, which is available to authorized users.

C. Bai · S. Tang · C. Bai (✉)  
Tourism and Food College, Shanghai Business School,  
Shanghai 200235, China  
e-mail: baichen\_bs@163.com

X. Chen  
Department of Chemistry and Institutes of Biomedical Sciences,  
Fudan University, Shanghai 200433, China

X. Chen (✉)  
Department of Biochemistry and Biophysics, University  
of North Carolina at Chapel Hill, UNC School of Medicine,  
120 Mason Farm Road, Genetic Medicine Building, Ste 3010,  
CB # 7260, Chapel Hill, NC 27599-7260, USA  
e-mail: xianc@email.unc.edu

## Introduction

Hepatocellular carcinoma (HCC) is the fifth most common cancer and the third most common cause of cancer-related death worldwide (Parkin et al. 2000). Because of the uncharacterized mechanisms of hepatocellular carcinogenesis, as well as the lack of effective strategies for HCC-specific therapeutic intervention, the 5-year survival rate of HCC patients is extremely low (Bosch et al. 2004).

14-3-3 proteins, the abundant, 28–33 kDa acidic polypeptides, belong to a family of conserved regulatory molecules found in all eukaryotic organisms (Aitken 2006). In mammals, seven isoforms encoded by seven distinct genes

have been identified ( $\beta$ ,  $\gamma$ ,  $\varepsilon$ ,  $\eta$ ,  $\sigma$ ,  $\tau$ , and  $\zeta$ ). Through interaction with close to 200 target proteins identified so far, those 14-3-3 isoforms are known to be involved in the regulation of the central BPs/pathways, including intracellular signaling, cell cycle control, apoptosis, stress response, proliferation, gene expression, and cytoskeletal integrity (Fu et al. 2000; Coblitz et al. 2006; van Heusden 2005; van Hemert et al. 2001). The diverse 14-3-3 interactors include protein kinases, transcription factors, biosynthetic enzymes, signaling molecules, apoptosis factors, tumor suppressors, and cytoskeletal proteins (van Heusden 2005; Morrison 2009). 14-3-3 proteins binding to the target protein can variably modify the function of their targets, such as alteration of their catalytic activity, DNA-binding activity, subcellular localization, protein–protein interactions, and their susceptibility to proteases and phosphatases (Hermeking 2003).

Many of the 14-3-3 binding partners are involved in cell cycle control, signaling, and apoptosis, suggesting the role of 14-3-3 proteins in carcinogenesis and tumor growth. The alteration of the level of 14-3-3 proteins has been associated with several human cancers. For example, the down-regulation of 14-3-3 $\sigma$ , primarily by CpG methylation, has been associated with a multitude of human epithelial cancers, indicating that 14-3-3 $\sigma$  acts as a tumor suppressor (Wilker and Yaffe 2004; Hermeking 2003). In HCC, the up-regulation of 14-3-3 $\varepsilon$  has been observed to be correlated with the high risk of tumor metastasis and poor survival of HCC patients (Ko et al. 2011). However, the detailed actions of 14-3-3 $\varepsilon$  in HCC are largely unknown.

Protein–protein interactions (PPIs) are the basic operators in biological processes. The systematic dissection of the protein–protein interaction network is not only essential for the understanding of HCC pathology, but also for screening the potential targets for cancer therapy. In our previous work, we dissected the 14-3-3 $\varepsilon$  interactome formed during the DNA damage response in HCC cells using amino acid-coded mass tagging [AACT, known by others as SILAC (Ong et al. 2003)]-based quantitative proteomic approach (Tang et al. 2013b). In this study, we employed a similar proteomic approach to profile/identify the 14-3-3 $\varepsilon$  interactome formed in native HCC cells. Twenty-nine proteins were identified as native 14-3-3 $\varepsilon$  interactors. Functional categorization and data-dependent network analysis revealed that 14-3-3 $\varepsilon$ , via association with these interactors, is involved in the regulation of diverse BPs/pathways, including cell cycle and apoptosis, signal transduction, cell adhesion, carbohydrate metabolism, nucleic acid metabolism, and intracellular transport, indicating that 14-3-3 $\varepsilon$  coordinates the cross-talk among these BPs/pathways to affect the survival, proliferation, and metastasis of HCC. The following biological validation demonstrated that 14-3-3 $\varepsilon$  indeed interacts with the key

modules (TAK1, PRPS1, YWHAQ, ACTN4) in each BP/ pathway, further supporting the role of 14-3-3 $\varepsilon$  in the tumorigenesis of HCC. This study, together with our previous findings, contributes to the body of knowledge regarding the 14-3-3 $\varepsilon$  interaction network in HCC cells, which would be valuable in providing the potential targets for HCC therapy.

## Materials and methods

### Chemicals and reagents

Dialyzed FBS (26400-044) and Lipofectamine 2000 (11668-019) were obtained from Invitrogen; Deuterium-labeled leucine (5,5,5-d<sub>3</sub> (Leu-d<sub>3</sub>), DLM-1259) was obtained from Cambridge Isotope Laboratories (CIL); Leucine-deficient RPMI 1640 medium was obtained from US Biological (R8999-03); Sequencing-grade trypsin (V5113) was purchased from Promega; and G418 sulfate (345810) was purchased from Calbiochem.

FLAG antibody (SG4130-29) was purchased from Shanghai Genomics, Shanghai, China; anti-FLAG beads (A2220) and 1 $\times$  FLAG peptide (F3290) were obtained from Sigma-Aldrich; and antibodies against PRPS1 (15549-1-AP), YWHAQ (14-3-3 $\theta$ , 14503-1-AP), ACTN4 (19096-1-AP),  $\beta$ -actin (60008-2-Ig), and MAP3K7 (TAK1, 12330-2-AP) were obtained from Proteintech.

### Cell culture, selection of stable HCC cell line

The HCC cell line QGY-7703 was purchased from the Cell Bank of Chinese Academy of Science and grown in RPMI 1640 medium supplemented with 10 % FBS (PAA Laboratories, A15-151).

The empty vector pcDNA 3.1 was transfected into QGY-7703 cells using Lipofectamine 2000 according to the manufacturer's protocol. The stable cell line was obtained by selecting the transfected cells using 400  $\mu$ g/ml G418. Stable HCC cells-expressing FLAG-14-3-3 $\varepsilon$  were used as described previously (Tang et al. 2013b).

### Stable isotope labeling (AACT/SILAC), isolation/ purification of 14-3-3 $\varepsilon$ interacting complexes assembled in native HCC cells

The control cells (vector only) were labeled with RPMI 1640 medium containing Leu-d<sub>3</sub>. The procedure of using Leu-d<sub>3</sub> to label the cellular proteome has been described previously (Yang et al. 2010; Wang et al. 2005; Zuo et al. 2010; Tang et al. 2013b).

Stable FLAG-14-3-3 $\varepsilon$ -expressing HCC cells were grown in regular RPMI 1640 medium (light), whereas

control cells were maintained in the medium containing Leu-d<sub>3</sub> (heavy). Each cell pool was lysed with lysis buffer (Beyotime, P0013) supplemented with protease inhibitor cocktail (Roche, 04693132001) and phosphatase inhibitor cocktail (Sigma-Aldrich, P0044), respectively. The protein concentration was quantified using Bradford assay (Beyotime, P0006) and mixed with 1:1 based on the total protein mass. Then, 400  $\mu$ l of anti-FLAG beads (Sigma-Aldrich, A2220) was added and incubated at 4 °C for 4 h to immunoprecipitate the FLAG-14-3-3 $\epsilon$  interacting proteins. After immunoprecipitation, anti-FLAG beads were washed five times with TBS buffer (50 mM Tris-HCl, pH 7.4, 150 mM NaCl) to eliminate the non-specific binding. The immunoprecipitates were eluted by 100  $\mu$ g/ml of FLAG peptide, and the eluates were concentrated to the appropriate volume for the following SDS-PAGE separation and Coomassie brilliant blue (CBB) staining.

#### Band excision, in-gel trypsin digestion, and peptide extraction

Following the protocol described previously (Shevchenko et al. 2006), the visible bands on the SDS-PAGE gel were excised. The gel slices were washed with Milli-Q water, and CBB dye was removed with 50 % acetonitrile (ACN)/50 mM ammonium bicarbonate for 15 min. The gel slices were dehydrated twice in 100 % ACN for 30 min and reconstituted overnight at 37 °C with an in-gel digestion reagent containing 12.5 ng/ $\mu$ l sequencing-grade trypsin (Promega, V5113). The tryptic peptides were extracted from the gel pieces with 50 % ACN/0.1 % TFA and lyophilized.

#### LC-MS/MS analysis

LC-MS analysis was performed on a nano-acquity UPLC system (Waters Corporation, Milford, USA) connected to an LTQ Orbitrap mass spectrometer (Thermo Scientific, Bremen, Germany) equipped with an online nano-electrospray ion source (Michrom Bioresources, Auburn, USA). Peptides were resuspended with 12  $\mu$ l of solvent A (5 % ACN, 0.1 % formic acid in water). 10  $\mu$ l of peptide solution was loaded onto the Captrap Peptide column (2  $\times$  0.5 mm, Michrom Bioresources, Auburn, USA) with a 20  $\mu$ l/min flow rate of solvent A for 5 min and then was separated on a Magic C18AQ reverse phase column (100  $\mu$ m id  $\times$  15 cm, Michrom Bioresources, Auburn, USA) with a three-step linear gradient. The gradient started from 5 % B (90 % ACN, 0.1 % formic acid in water) to 45 % B over 100 min, increased to 80 % B over 3 min, and then to 5 % B over 2 min. The column was re-equilibrated at initial conditions for 15 min. The column flow rate was maintained at 500 nl/min and the column temperature was

maintained at 35 °C. The electrospray voltage of 1.8 kV versus the inlet of the mass spectrometer was used.

The LTQ Orbitrap mass spectrometer was operated in the data-dependent mode to switch automatically between MS and MS/MS acquisition. Survey full-scan MS spectra with one microscan ( $m/z$  400–2,000) were acquired in the Orbitrap with a mass resolution of 60,000 at  $m/z$  400, followed by MS/MS of the eight most-intense peptide ions in the LTQ analyzer. The automatic gain control (AGC) was set to 1,000,000 ions, with a maximum accumulation time of 500 ms. For MS/MS, we used an isolation window of 2  $m/z$  and the automatic gain control (AGC) of LTQ was set to 20,000 ions, with a maximum accumulation time of 120 ms. Single charge state was rejected and dynamic exclusion was used with two microscans in 10 and 90 s exclusion duration. For MS/MS, precursor ions were activated using 35 % normalized collision energy at the default activation  $q$  of 0.25 and an activation time of 30 ms. The spectra were recorded with Xcalibur (version 2.2.0) software.

The MS raw data and the related files can be found at PeptideAtlas (<http://www.peptideatlas.org/PASS/PASS00373>).

#### Protein identification and quantification

The raw mass spectra files were processed using MaxQuant software (version 1.4.0.8, <http://www.maxquant.org/>) (Cox and Mann 2008). Data were searched using the Andromeda search engine (Cox et al. 2011) against the IPI human database (v3.68, 87,061 entries). The parameters for database search were set as follows: (1) The minimum required peptide length was 7 amino acids. (2) Trypsin cleavage specificity was applied with up to two missed cleavages allowed. (3) Various modifications included methionine oxidation (15.9994 Da), N-acetylation of protein N-termini (42.0106 Da), and leu-d<sub>3</sub> (3.0188 Da). (4) Initial mass deviation of the precursor ion and fragment ions were up to 10 ppm and 0.5 Da, respectively. (5) The false discovery rate (FDR) was set to 1 % at both the peptide and protein levels. (6) Only proteins sequenced with at least two peptides were considered as reliable identification.

Quantification of proteins (L/H ratio) was performed using MaxQuant (version 1.4.0.8). Briefly, (1) Leu and Leu-d<sub>3</sub> were selected as light (L) and heavy (H) labels, respectively. (2) Methionine oxidations and acetylation of protein N-termini were specified as variable modifications. (3) Peptide and protein FDRs were set to 0.01 and seven amino acids were required as minimum peptide length. (4) Unique and razor peptides were used for protein quantification. (5) The protein ratios (L/H) were automatically calculated and normalized by MaxQuant. (6) Specific interaction partners were determined by the significance

*B* value ( $<0.05$ ), which is the *p* value for detection of significant outlier protein ratios calculated on the protein subsets obtained by intensity binning (Cox and Mann 2008). Significance *B* can be calculated using the freely available Perseus analysis software (<http://www.perseus-framework.org/>).

#### Functional categorization and network analysis

The MS-identified 14-3-3 $\epsilon$  interactors were submitted to Gene Ontology (<http://www.geneontology.org/>) and DAVID (<http://www.david.abcc.ncifcrf.gov>) for categorization according to their previously known associations with different functions. Signaling pathways were classified using PANTHER (<http://www.pantherdb.org/>). Network analysis was performed using STRING mapping tool (<http://string-db.org/>). The 14-3-3 $\epsilon$  interacting network scheme was constructed using Cytoscape 2.8.3 (<http://www.cytoscape.org/>).

#### Co-immunoprecipitation and immunoblotting

The control cells and FLAG-14-3-3 $\epsilon$ -expressing cells ( $\sim 1 \times 10^7$  cells/each group) were lysed, and 40  $\mu$ l of anti-FLAG beads was added to perform immunoprecipitation at 4 °C for 3 h with gentle shaking. After immunoprecipitation, anti-FLAG beads were washed four times with TBS buffer (50 mM Tris-HCl, pH 7.4, 150 mM NaCl), and immunoprecipitates were eluted by directly boiling the beads.

Protein samples were separated using SDS-PAGE and transferred to PVDF membrane (Immobilon-P<sup>SQ</sup> Membrane, 0.2  $\mu$ m). The membranes were blocked with 5 % nonfat milk and probed with the specified primary antibodies followed by incubation with secondary antibody conjugated with horseradish peroxidase, and ECL substrate (Pierce, 34095) was subsequently added to the membrane and exposed using an ECL system.

## Results

#### Dissection of 14-3-3 $\epsilon$ interactome formed in native HCC cells

In our previous work, we generated a HCC cell line that stably expressed the FLAG-tagged 14-3-3 $\epsilon$ , and we dissected the HCC-specific 14-3-3 $\epsilon$  interactome formed during the DNA damage response using an AACT/SILAC-based quantitative proteomic approach (Tang et al. 2013b). In this study, using the similar method, we designed an experiment to profile/identify the 14-3-3 $\epsilon$  interactome formed in native HCC cells. Briefly (Fig. 1a), the FLAG-

14-3-3 $\epsilon$ -expressing HCC cells were grown in the “light” (L) medium, whereas the control cells (vector only) were maintained in “heavy” (H) medium containing Leu-d<sub>3</sub>. The proteins extracted from each group were mixed in a ratio of 1:1 based on the total protein mass, and anti-FLAG beads were added to immunoprecipitate the 14-3-3 $\epsilon$  interacting complex for the following SDS-PAGE separation (Fig. 1b), in-gel trypsin digestion, and LC-MS/MS analysis.

Based on the fact that leu-d<sub>3</sub> is 3 Da heavier than leu, in MS analysis, for each leu-containing peptide, a paired isotope signals with a mass split of  $3 n/z$  (*n* stands for the number of leu in the peptide and *z* is the charge number of the peptide) could be observed. The “light” isotope peak is from the FLAG-14-3-3 $\epsilon$ -expressing cells, and the “heavy” peak is from the control cells. The ratio of paired light versus heavy isotope signals (L/H) reflects the changes of the binding strength of a protein to 14-3-3 $\epsilon$ . For most non-specific contaminants, their L/H ratios should be close to 1.0. The proteins quantified with L/H ratios greater than 1.0 should be considered to be the specific 14-3-3 $\epsilon$  interactors.

According to the stringent criteria for protein identification and quantification (see Materials and methods), among a total of 743 protein identifications, 584 proteins were quantified with L/H ratios (Table S1). Using significance *B* value ( $p < 0.05$ ) as the threshold to distinguish the specific 14-3-3 $\epsilon$  interactors (Cox and Mann 2008), initially, 55 proteins were demonstrated as having significant abundance changes (L/H ratios  $>1.70$ ) (Fig. 2 and Table S2). However, we noted that certain highly abundant proteins, such as cytoskeletal/structural proteins, histones, hnRNP proteins, and ribosomal proteins, were included in this list. Based on the previous report (Trinkle-Mulcahy et al. 2008), they are in the class of “beads proteome”, i.e., proteins that often stick to the agarose beads where the FLAG antibody is conjugated to, therefore, co-purify with the “true” protein interacting partners during the process of immunoprecipitation. Thus, after excluding these proteins, 29 proteins were considered to be 14-3-3 $\epsilon$  interactors formed in native HCC cells (Table 1 and Table S2).

#### Functional categories of the identified 14-3-3 $\epsilon$ interacting proteins in native HCC cells

To clarify the BPs of the identified HCC-specific 14-3-3 $\epsilon$  interactors, we utilized Gene Ontology (<http://www.geneontology.org/>) and DAVID (<http://david.abcc.ncifcrf.gov/>) to classify these proteins on the basis of their known functions. As shown in Fig. 3a and Table 1, these 14-3-3 $\epsilon$  interactors were found in multiple functional categories/BPs, such as cell cycle and apoptosis, signal transduction, cell adhesion, carbohydrate metabolism, nucleic acid metabolism, and intracellular transport.

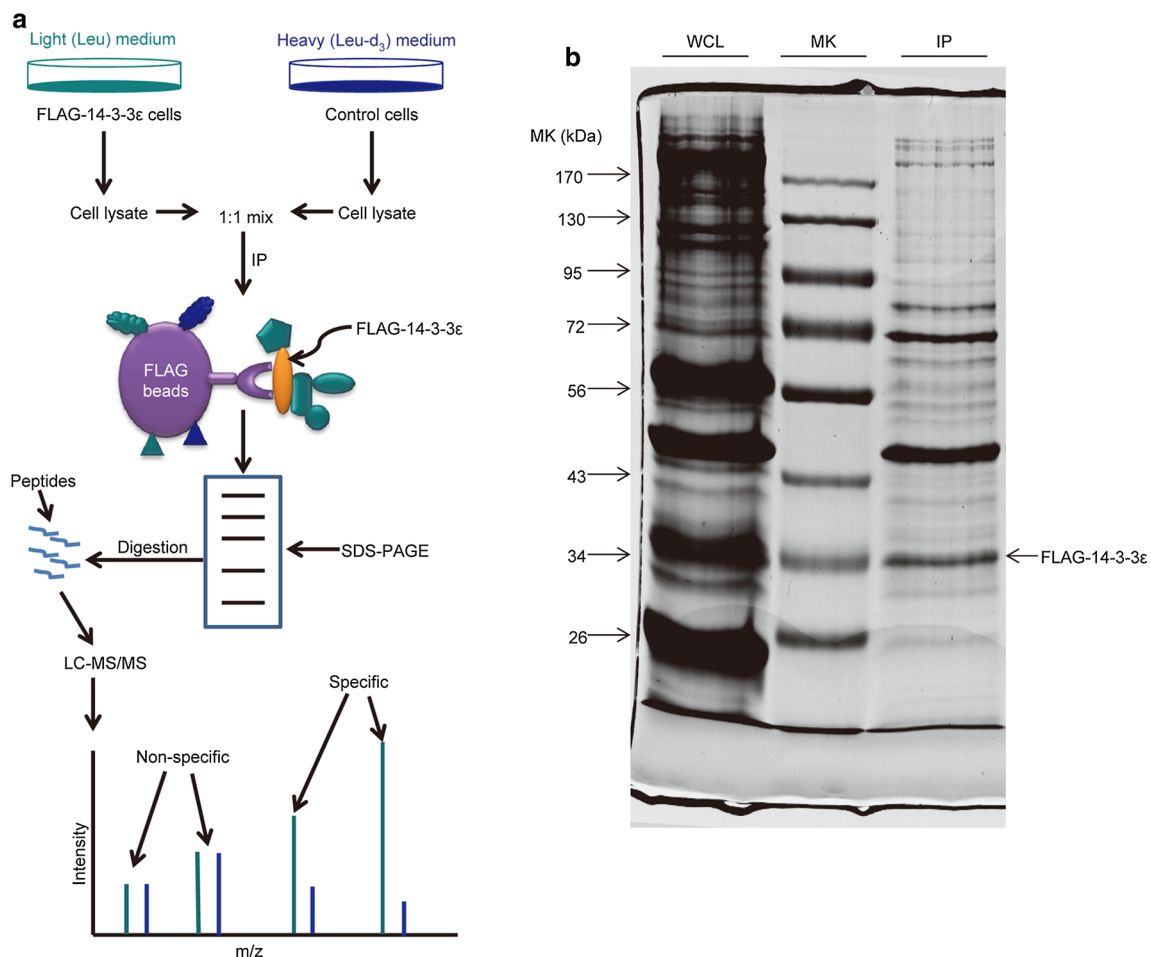


**Fig. 1** Isolation of native HCC-specific 14-3-3 $\epsilon$ -interacting complex by immunoprecipitation. **a** Strategy to identify 14-3-3 $\epsilon$ -interacting partners in native HCC cells. HCC cells stably expressing FLAG-14-3-3 $\epsilon$  were maintained in “light” medium (Leu). In parallel, control cells were grown in “heavy” medium (Leu- $d_3$ ). The whole cell lysates (WCL) derived from each cell pool were mixed 1:1 based on the total protein mass. The FLAG-14-3-3 $\epsilon$ -interacting complex was purified using anti-FLAG beads followed by SDS-PAGE separation,

in-gel trypsin digestion, and LC-MS/MS analysis. **b** Isolation of the 14-3-3 $\epsilon$  complex by immunoprecipitation. Purification of the 14-3-3 $\epsilon$  complex was carried out via the procedure described in “[Materials and methods](#)”. Proteins were separated on SDS-PAGE and stained with Coomassie brilliant blue (CBB). WCL whole cell lysates, IP immunoprecipitates, MK protein marker. Bait protein FLAG-tagged 14-3-3 $\epsilon$  is indicated by *arrow* on the SDS-PAGE gel

The distribution of the identified 14-3-3 $\epsilon$  interactors in these functional categories is given in Fig. 3a. One portion of the 14-3-3 $\epsilon$  interactor was 14-3-3 isoform ( $\beta$ ,  $\gamma$ ,  $\zeta$ ,  $\eta$ ,  $\theta$ ), which plays a key role in the regulation of cell cycle progression and apoptosis. For instance, 14-3-3 proteins interact with CDC25 to suppress G2/M cell cycle progression (Forrest and Gabrielli 2001; Peng et al. 1997), and interact with BAD (Zha et al. 1996; Datta et al. 2000) and BAX (Nomura et al. 2003; Samuel et al. 2001) to inhibit cellular apoptosis. Furthermore, the levels of 14-3-3 $\epsilon$  and  $\zeta$  were found to be up-regulated in HCC, and the up-regulation of these isoforms was correlated to the tumorigenesis of HCC (Ko et al. 2011; Niemantsverdriet et al. 2008). Together, these findings indicate the important role of 14-3-3 isoforms in carcinogenesis. In addition, 14-3-3

proteins often form homo- or hetero-dimers for function (Fu et al. 2000). In our MS-identified 14-3-3 $\epsilon$  interactome, five 14-3-3 isoforms were identified ( $\beta$ ,  $\gamma$ ,  $\zeta$ ,  $\eta$ ,  $\theta$ ), indicating that the FLAG-tagged 14-3-3 $\epsilon$  protein is functional, and also demonstrating the accuracy of our quantitative proteomic approach.

MAP3K7 (TAK1) is an evolutionarily conserved member of the MAPKKK family that plays key roles in the regulation of MAPKs and NF- $\kappa$ B signaling pathways to promote cell survival (Ninomiya-Tsuji et al. 1999; Sakurai et al. 1999; Lee et al. 2000; Yamaguchi et al. 1995). TAK1 requires a protein activator, MAP3K7IP1 (TAB1), to induce full activation (Shibuya et al. 1996). Our previous work demonstrated that both TAK1 and TAB1 are 14-3-3 $\epsilon$  interactors formed in HCC cells in response to DNA



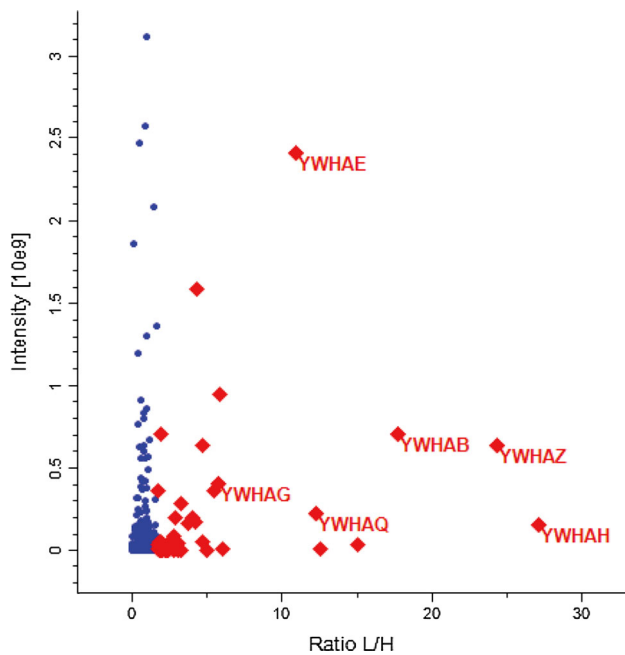


**Fig. 2** Proteome-wide accurate quantification and significance. Normalized protein ratios are plotted against protein intensities. The data points are colored by their “significance *B*”, with blue filled circles (526 proteins) having values  $>0.05$ , the ratios of these proteins are centered around 1.0, which are considered to be the non-specific binding. With red filled diamonds (56 proteins) having values  $<0.05$ , the ratios of these proteins are  $>1.70$ , which are considered as the specific 14-3-3 $\epsilon$  interactors. Some known 14-3-3 $\epsilon$  interactors (YWHAG, YWHAQ, YWHAB, YWHAZ, and YWHAH) are indicated (color figure online)

damage, and 14-3-3 $\epsilon$  negatively regulates the anti-apoptotic activity of TAK1 (Tang et al. 2013b). Our findings are consistent with the observations, clearly indicating that 14-3-3 $\epsilon$  integrates with TAK1 signaling pathways to determine the HCC cell fate.

Alpha-actinins (ACTN1 and ACTN4) are cytoskeletal proteins that bind actin filaments to maintain cytoskeletal structure and cell morphology (Djinovic-Carugo et al. 2002). Recently, some work demonstrated that alpha-actinins act as nuclear receptor coactivators that promote cell proliferation (Khurana et al. 2011; Babakov et al. 2008). ACTN1 and ACTN4 were identified as 14-3-3 $\epsilon$  interactors, indicating that 14-3-3 $\epsilon$  via associations with these proteins regulates the proliferation and motility (metastasis) of HCC.

The largest portion of the 14-3-3 $\epsilon$  interactome in HCC cells was represented by proteins involved in nucleic acid metabolism. The highlighted one is ribose-phosphate pyrophosphokinase (PRPS). Human PRPS exists as complexes containing PRPS1, PRPS2 and two associated proteins (PRPSAP1 and PRPSAP2) (Kita et al. 1989, 1994; Sonoda et al. 1997). PRPS controls purine metabolism and nucleotide biosynthesis, which affects cell growth and proliferation (Tatibana et al. 1995). A prior study indicated

that PRPS1 associates with p300 to regulate DNA synthesis (Kaida et al. 2005). Components of the PRPS complex have been identified as 14-3-3 $\epsilon$  interactors in different cell lines as indicated by our previous work (Zuo et al. 2010; Tang et al. 2013b). These previous results, along with the identification in the present study, indicate that 14-3-3 $\epsilon$  may coordinate with PRPS to modulate DNA synthesis and the subsequent cell growth and proliferation of HCC.

Elevated glucose catabolism is important for the production of energy and required anabolic precursors in rapidly growing tumor (Shaw 2006). The up-regulation of glucose-6-phosphate dehydrogenase (G6PD) has been observed to be correlated with the progression of HCC and other tumors (Premalatha et al. 1997; Sivanesan and Begum 2007). G6PD, identified as 14-3-3 $\epsilon$  interactor, may indicate that 14-3-3 $\epsilon$  integrates into glucose metabolism pathways to regulate the growth of HCC.

Data-dependent network analysis of 14-3-3 $\epsilon$  interacting proteins reveals that 14-3-3 $\epsilon$  coordinates the cross-talk among diverse pathway modules

To elucidate how 14-3-3 $\epsilon$  coordinates multiple functional pathways in the tumor environment and the possible functional role of the 14-3-3 $\epsilon$  interactome in HCC, we utilized the STRING interaction network mapping tool (<http://string-db.org/>) and PANTHER pathway mapping tool (<http://www.pantherdb.org/>) to explore the interconnected relationships among the 14-3-3 $\epsilon$  interactors and further identified each different pathway module. As shown in Fig. 3b, 14-3-3 $\epsilon$  was determined to be the critical network node inter-connecting multiple BPs/pathways associated with tumor growth, proliferation, and metastasis, including EGF receptor/PI3K signaling pathway, MAPKs/inflammatory signaling pathways, integrin pathway, nucleotide metabolism, and protein transport.

In HCC, the disorder of multiple signaling pathways associated with cell proliferation and survival has been elucidated. The up-regulation of epidermal growth factor (EGF), transforming growth factor (TGF), fibroblast growth factor (FGF), as well as EGF receptor (EGFR) and platelet-derived growth factor receptor (PDGFR) has been observed in HCC cell lines and tissues (Thomas and Abbruzzese 2005). Furthermore, downstream of these receptors, the imbalance of Ras/Raf/MEK/ERK and PI3K/AKT signaling cascades were also characterized in HCC (Thomas and Abbruzzese 2005; Mendez-Sanchez et al. 2008). 14-3-3 $\epsilon$  and its isoforms have been well characterized in association with the key modules [e.g., RAF, PI3K, AKT, MAP3K7, and BAD (Morrison 2009; van Hemert et al. 2001; Wilker and Yaffe 2004; Tang et al. 2013b)] involved in these pathways. In the network, 14-3-3 $\epsilon$  clearly integrates into these pathways, indicating that 14-3-3 $\epsilon$

**Table 1** The native HCC-specific 14-3-3ε interactors and their associations with different biological processes

IPI no.	Gene name	Protein name	Pep <sup>a</sup>	L/H ratio <sup>b</sup>	Variability (%) <sup>c</sup>
IPI00000816	YWHAЕ	14-3-3 protein epsilon (bait)	16	10.89	119.6
Cell cycle and apoptosis					
IPI00018146	YWHAQ	14-3-3 protein theta	8	12.31	40.69
IPI00021263	YWHAZ	14-3-3 protein zeta	14	24.38	98.07
IPI00216319	YWHAH	14-3-3 protein eta	7	27.10	84.83
IPI00759832	YWHAB	14-3-3 protein beta	7	17.74	68.87
IPI00910779	YWHAG	14-3-3 protein gamma	6	5.75	34.28
Signal transduction					
IPI00218566	MAP3K7	Isoform 1A of Mitogen-activated protein kinase kinase kinase 7	5	2.16	14.25
IPI00019459	MAP3K7IP1	Mitogen-activated protein kinase kinase kinase 7-interacting protein 1	8	1.76	40.01
Cell adhesion					
IPI00013508	ACTN1	Alpha-actinin-1	39	2.88	30.81
IPI00013808	ACTN4	Alpha-actinin-4	48	4.72	48.33
IPI00291175	VCL	Isoform 1 of vinculin	10	1.87	43.48
IPI00854700	KIAA1598	Isoform 1 of shootin-1	3	2.02	29.48
IPI00005087	TMOD3	Tropomodulin-3	14	2.77	28.21
Carbohydrate metabolic process					
IPI00006682	PPP1R3D	Protein phosphatase 1 regulatory subunit 3D	4	12.54	49.28
IPI00220808	PFKFB2	6-Phosphofructo-2-kinase/fructose-2,6-biphosphatase 2	5	1.94	29.31
IPI00645745	G6PD	Glucose-6-phosphate dehydrogenase	4	2.32	79.47
IPI00909143	DLD	Dihydrolipoyl dehydrogenase	5	2.69	125.37
Nucleic acid metabolic process					
IPI00003168	PRPSAP2	Phosphoribosyl pyrophosphate synthetase-associated protein 2	16	5.82	48.30
IPI00797603	PRPSAP1	Phosphoribosyl pyrophosphate synthetase-associated protein 1	15	5.42	42.39
IPI00219616	PRPS1	Ribose-phosphate pyrophosphokinase 1	10	3.75	29.88
IPI00219617	PRPS2	Isoform 1 of Ribose-phosphate pyrophosphokinase 2	12	4.33	56.37
IPI00029054	NT5C2	Cytosolic purine 5-nucleotidase	7	6.04	54.58
IPI00014319	IVNS1ABP	Influenza virus NS1A-binding protein	11	3.24	24.18
IPI00161600	C1orf79	Cooperator of PRMT5	3	1.96	20.22
Intracellular transport					
IPI00001639	KPNB1	Importin subunit beta-1	2	2.80	55.98
IPI00411426	VPS26A	Vacuolar protein sorting-associated protein 26A	3	1.94	19.32
IPI00908710	SQSTM1	Sequestosome-1	3	2.34	19.09
Others					
IPI00910095	C1orf27	Odorant response abnormal 4 isoform 3	3	2.48	20.22
IPI00465370	RNF219	RING finger protein 219	3	1.85	3.94
IPI00479893	C10orf18	Isoform 2 of uncharacterized protein C10orf18	2	2.01	90.78

<sup>a</sup> Peptide number matched to the protein<sup>b</sup> Protein abundance changes enriched by 14-3-3ε from FLAG-14-3-3ε-expressing cells vs. control cells<sup>c</sup> Variability was calculated by the isotope intensity ratio from multiple leucine-containing peptides

plays a critical role in the regulation of proliferation, differentiation, and survival of HCC.

Another subnetwork that 14-3-3ε participated in is the integrin pathway. Invasion and metastasis are important determinants in the progression of HCC (Quaranta 2002). Integrin protein family plays principal roles in the processes of growth, differentiation, and invasion and

metastasis of malignant cells (Dedhar and Hannigan 1996). The alteration of the level of integrins has been demonstrated in HCC with an aggressive phenotype (Jaskiewicz and Chasen 1995; Yao et al. 1997). Prior studies revealed that 14-3-3 proteins interact with several integrin isoforms to enhance cell spreading and mobility (Han et al. 2001; Santoro et al. 2003). In addition, α-actinin-4 (ACTN4) was

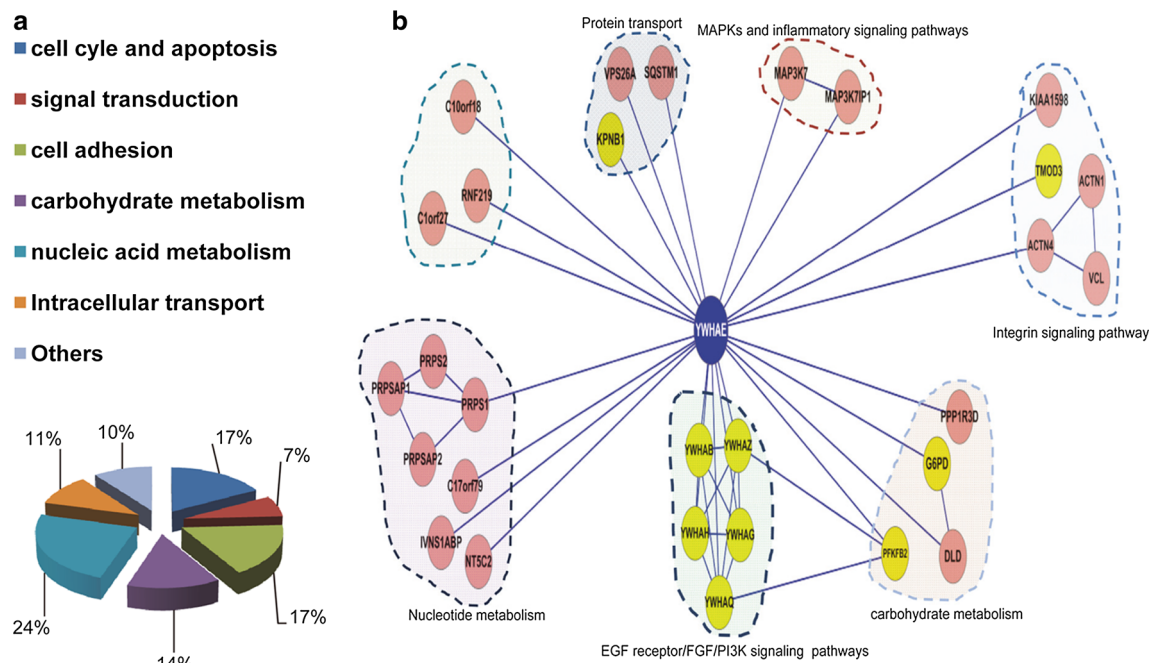


**Fig. 3** Functional categorization and network analysis of the native HCC-specific 14-3-3ε interactome. **a** Functional categories and the corresponding percentage of the native 14-3-3ε-interacting partners identified by quantitative proteomic approach. The 14-3-3ε interactors were categorized according to their known involvements in various biological processes (BPs) using online bioinformatics analysis tools such as gene ontology (<http://www.geneontology.org/>) and DAVID (<http://www.david.abcc.ncifcrf.gov>), and then the corresponding

percentage of those interactors involved in different BPs were plotted. **b** Data-dependent network analysis of 14-3-3ε interactors. The gene symbol of 14-3-3ε is YWHAE. Signaling pathways were classified using PANTHER (<http://www.pantherdb.org/>); the network was constructed by the bioinformatics analysis tool: STRING (<http://string.embl.de/>). The links in the network were edited using Cytoscape 2.8.3 (<http://www.cytoscape.org/>). Some known 14-3-3ε interactors were marked in yellow circles (color figure online)

demonstrated to be recruited to the integrin complex to regulate cell migration (Byron et al. 2012). These clues indicate that 14-3-3ε, via association with integrin and actinin, is involved in the regulation of invasion and metastasis of HCC.

In the network, 14-3-3ε was also demonstrated to be integrated into the processes of nucleotide metabolism and carbohydrate metabolism, suggesting that 14-3-3ε coordinates the processes of DNA synthesis and energy generation to regulate the growth of HCC.

In summary, this data-dependent network analysis provided further support that 14-3-3ε coordinates multiple pathways to regulate cell growth, differentiation, cell cycle progression, and invasion and metastasis in HCC.

Validation of the HCC-specific 14-3-3ε interactome dataset using immunoprecipitation/immunoblotting

We used co-immunoprecipitation (co-IP) and concurrent immunoblotting to evaluate the physiologically relevant accuracy of our proteomics dataset of the HCC-specific 14-3-3ε interacting complex. As shown in Fig. 4 and Fig. S1, consistent with MS quantification (Fig. S1), 14-3-30 (YWHAQ), ACTN4, PRPS1, and MAP3K7 (TAK1) were

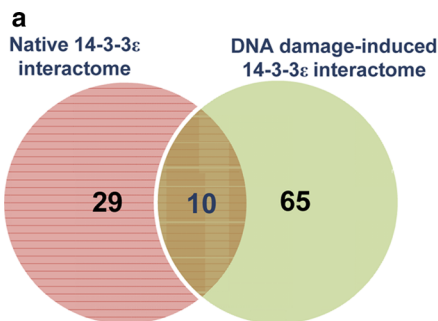
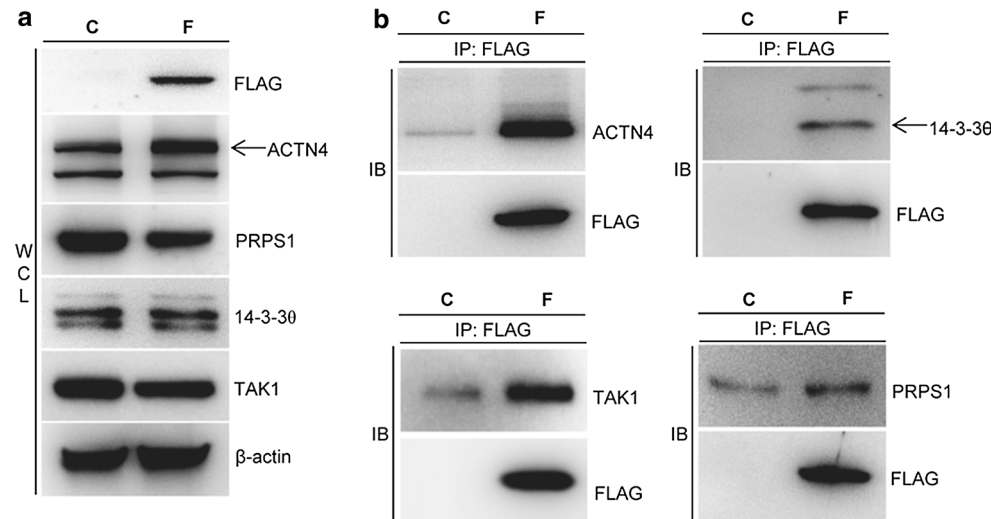
confirmed as 14-3-3ε interactors. These results clearly support the accuracy of the MS-identified 14-3-3ε interactome dataset. The biological validation data, together with data-dependent network analysis (Fig. 3), indeed demonstrated that 14-3-3ε associates with these modules involved in each BPs/pathways to regulate the proliferation, survival, and metastasis of HCC.

Statistical analysis of HCC-specific 14-3-3ε interactomes formed under different conditions

In our previous work, we obtained 65 HCC-specific 14-3-3ε interactors formed during the DNA damage response (Tang et al. 2013b). In the present study, we identified 29 14-3-3ε interactors formed in native HCC cells. In the comparison of these two datasets, 10 proteins were identified in both, indicating that these proteins may be the constitutive 14-3-3ε interactors in HCC cells (Fig. 5a, b). Excluding the redundant proteins, in total, 84 proteins were identified as 14-3-3ε interacting partners in HCC cells, which is in agreement with the nature of 14-3-3 proteins via associations with hundreds of proteins regulating diverse cellular processes as previously reported (Thomas et al. 2005; Coblitz et al. 2006).



**Fig. 4** Immunoblotting validation of the MS-identified 14-3-3ε interactors. The cell lysates were immunoprecipitated (IP) with anti-FLAG beads and the IP eluates were then analyzed by immunoblotting (IB) against the indicated antibodies. **a** Whole cell lysate (WCL). **b** Immunoblotting analysis of the indicated proteins in 14-3-3ε complex pulled-down by anti-FLAG beads. *C* control cell, *F* FLAG-14-3-3ε-expressing cell



**b**

IPI Number	Gene Symbol
IPI00001639	KPNB1
IPI00003168	PRPSAP2
IPI00797603	PRPSAP1
IPI00219617	PRPS2
IPI00005087	TMOD3
IPI00013808	ACTN4
IPI00014319	IVNS1ABP
IPI00218566	MAP3K7
IPI00019459	MAP3K7IP1
IPI00029054	NT5C2

**c**

Biological validation		
Dataset	Native 14-3-3ε interactome	DNA damage-induced 14-3-3ε interactome
Validation	4	8
Proteins	YWHAQ, ACTN4, MAP3K7(TAK1) <sup>a</sup> , PRPS1	YWHAZ, HDAC1, HDAC6, NONO, DDB1, MAP3K7 (TAK1) <sup>a</sup> , MAP3K7IP1 (TAB1), MVP <sup>b</sup>

**Fig. 5** Statistical analysis of condition-based 14-3-3ε interactome formed in HCC. **a–b** Analysis of HCC-specific 14-3-3ε interactome formed in native condition and DNA damage-induced condition. Our prior study identified sixty-five 14-3-3ε interacting partners (DNA damage-induced 14-3-3ε interactome) (Tang et al. 2013b). In the present study, twenty-nine 14-3-3ε interactors were identified in

native HCC cells (native 14-3-3ε interactome). Ten proteins were identified in both datasets (**a**) and listed (**b**). **c** The summary of HCC-specific 14-3-3ε interactors with biological validation. **a** MAP3K7 (TAK1) were both identified and validated in two datasets. **b** See in reference (Tang et al. 2013a)

In terms of biological validation, in total, 11 proteins were confirmed as 14-3-3 $\epsilon$  interactors using immunoprecipitation/immunoblotting (Fig. 5c). Notably, most of these validated proteins are new 14-3-3 $\epsilon$  interactors in comparison with the known protein–protein interaction database (Biogrid, <http://thebiogrid.org/>; HPRD, <http://hprd.org/>, and other such tools). More importantly, some of them [TAK1 (Tang et al. 2013b), MVP (Tang et al. 2013a)] were conducted in depth to explore the detailed interaction mechanisms with 14-3-3 $\epsilon$ . Taken together, these findings provide extensive evidence of the 14-3-3 $\epsilon$  interactome in HCC so far, which should be the critical reference for understanding the pathology of HCC and therapeutic intervention of HCC through interfering with specific protein–protein interactions.

## Discussion

14-3-3 proteins, the evolutionarily conserved regulatory molecules, have been found in all eukaryotic organisms (Aitken 2006). In mammals, seven 14-3-3 isoforms that are encoded by distinct genes were identified. Although there is relatively high sequence homology that all 14-3-3 isoforms share, the proteomic screening using various 14-3-3 isoforms as bait proteins revealed the isomer-specific composition of the interactome of different 14-3-3 family members (Pozuelo Rubio et al. 2004; Meek et al. 2004; Jin et al. 2004; Benzinger et al. 2005), indicating that individual 14-3-3 isoforms may play specific biological roles.

Given that 14-3-3 proteins regulate diverse biological processes, accumulating evidence from cell and animal models, as well as patient samples, has established a strong link between 14-3-3 proteins and many types of cancer (Morrison 2009; Hermeking 2003; Tzivion et al. 2006). The 14-3-3 $\sigma$  is directly connected to human cancer. Gene silencing of 14-3-3 $\sigma$ , mainly by CpG methylation, occurs in numerous solid tumor types and even in hematologic malignancies (Lodygin and Hermeking 2005), suggesting that 14-3-3 $\sigma$  has tumor suppressing activity. In support of a pro-oncogenic role of 14-3-3, the up-regulation of 14-3-3 $\zeta$  and  $\epsilon$  is associated with poor prognosis of breast cancer and HCC patients, respectively (Neal et al. 2009; Ko et al. 2011). Other isoforms, including  $\beta$ ,  $\gamma$ , and  $\tau$ , have also been observed to be up-regulated in cancer specimens (Qi et al. 2005, 2007; Pereira-Faca et al. 2007). Although the connection between 14-3-3 and cancer development has been established, further studies to elucidate the mechanisms by which each isoform of 14-3-3 contributes to tumorigenesis are required.

Given that 14-3-3 $\epsilon$  plays an important role in HCC carcinogenesis, in this study, we employed AACT/SILAC-based quantitative proteomic approach to profile/identify the 14-3-3 $\epsilon$  interactome formed in native HCC cells in a

systems view. Functional categorization and data-dependent network analysis of the 14-3-3 $\epsilon$  interactors revealed that 14-3-3 $\epsilon$  is not only involved in the regulation of the known BPs/pathways such as cell cycle and apoptosis, signal transduction, and intracellular transport, but also in the regulation of carbohydrate metabolic process, cell adhesion, and nucleic acid metabolic process in HCC cells. The subsequent biological validation further supports that 14-3-3 $\epsilon$ , by interacting with the key modules involved in the specific BPs/pathways, coordinates their cross-talk, therefore regulating the proliferation, survival, and metastasis of HCC cells.

Our previous work used the similar proteomic approach to profile/identify the 14-3-3 $\epsilon$  interactome of HCC in response to DNA damage (Tang et al. 2013b). Together with the findings obtained in the present study, we dissected the 14-3-3 $\epsilon$  interactome in HCC cells in depth, and our findings should be useful in providing potential targets for HCC intervention.

**Acknowledgments** The present study was supported by Shanghai Knowledge and Resource Center for Commerce and Trade Service Industry (ZF1226). This work was also supported, in part, by the grants from Shanghai Science and Technology Development Program (Grants 03DZ14024 and 07ZR14010) and the 863 High Technology Foundation of China (Grant 2006AA02A310). This work was also supported in part by National Institutes of Health (NIH) grants to X.C. (NIH R01AI064806 and NIH 1U24CA160035).

**Conflict of interest** The authors declare that they have no conflict of interest.

## References

- Aitken A (2006) 14-3-3 proteins: a historic overview. *Semin Cancer Biol* 16(3):162–172. doi:10.1016/j.semcancer.2006.03.005
- Babakov VN, Petukhova OA, Turoverova LV, Kropacheva IV, Tentler DG, Bolshakova AV, Podolskaya EP, Magnusson KE, Pinaev GP (2008) RelA/NF-kappaB transcription factor associates with alpha-actinin-4. *Exp Cell Res* 314(5):1030–1038. doi:10.1016/j.yexcr.2007.12.001
- Benzinger A, Muster N, Koch HB, Yates JR 3rd, Hermeking H (2005) Targeted proteomic analysis of 14-3-3 sigma, a p53 effector commonly silenced in cancer. *Mol Cell Proteomics* 4(6):785–795. doi:10.1074/mcp.M500021-MCP200
- Bosch FX, Ribes J, Diaz M, Cléries R (2004) Primary liver cancer: worldwide incidence and trends. *Gastroenterology* 127(5 Suppl 1):S5–S16. doi:10.1053/j.gastro.2004.09.011
- Byron A, Humphries JD, Craig SE, Knight D, Humphries MJ (2012) Proteomic analysis of alpha4beta1 integrin adhesion complexes reveals alpha-subunit-dependent protein recruitment. *Proteomics* 12(13):2107–2114. doi:10.1002/pmic.201100487
- Coblitz B, Wu M, Shikano S, Li M (2006) C-terminal binding: an expanded repertoire and function of 14-3-3 proteins. *FEBS Lett* 580(6):1531–1535. doi:10.1016/j.febslet.2006.02.014
- Cox J, Mann M (2008) MaxQuant enables high peptide identification rates, individualized p.p.b.-range mass accuracies and proteome-wide protein quantification. *Nat Biotechnol* 26(12):1367–1372. doi:10.1038/nbt.1511

- Cox J, Neuhauser N, Michalski A, Scheltema RA, Olsen JV, Mann M (2011) Andromeda: a peptide search engine integrated into the MaxQuant environment. *J Proteome Res* 10(4):1794–1805. doi:[10.1021/pr101065j](https://doi.org/10.1021/pr101065j)
- Datta SR, Katsov A, Hu L, Petros A, Fesik SW, Yaffe MB, Greenberg ME (2000) 14-3-3 proteins and survival kinases cooperate to inactivate BAD by BH3 domain phosphorylation. *Mol Cell* 6(1):41–51. doi:[10.1016/S1097-2765\(05\)00012-2](https://doi.org/10.1016/S1097-2765(05)00012-2)
- Dedhar S, Hannigan GE (1996) Integrin cytoplasmic interactions and bidirectional transmembrane signalling. *Curr Opin Cell Biol* 8(5):657–669. doi:[10.1016/S0955-0674\(96\)80107-4](https://doi.org/10.1016/S0955-0674(96)80107-4)
- Djinovic-Carugo K, Gautel M, Ylanne J, Young P (2002) The spectrin repeat: a structural platform for cytoskeletal protein assemblies. *FEBS Lett* 513(1):119–123. doi:[10.1016/S0014-5793\(01\)03304-X](https://doi.org/10.1016/S0014-5793(01)03304-X)
- Forrest A, Gabrielli B (2001) Cdc25B activity is regulated by 14-3-3. *Oncogene* 20(32):4393–4401. doi:[10.1038/sj.onc.1204574](https://doi.org/10.1038/sj.onc.1204574)
- Fu H, Subramanian RR, Masters SC (2000) 14-3-3 proteins: structure, function, and regulation. *Annu Rev Pharmacol Toxicol* 40:617–647. doi:[10.1146/annurev.pharmtox.40.1.617](https://doi.org/10.1146/annurev.pharmtox.40.1.617)
- Han DC, Rodriguez LG, Guan JL (2001) Identification of a novel interaction between integrin beta1 and 14-3-3beta. *Oncogene* 20(3):346–357. doi:[10.1038/sj.onc.1204068](https://doi.org/10.1038/sj.onc.1204068)
- Hermeking H (2003) The 14-3-3 cancer connection. *Nat Rev Cancer* 3(12):931–943. doi:[10.1038/nrc1230](https://doi.org/10.1038/nrc1230)
- Jaskiewicz K, Chasen MR (1995) Differential expression of transforming growth factor alpha, adhesions molecules and integrins in primary, metastatic liver tumors and in liver cirrhosis. *Anticancer Res* 15(2):559–562
- Jin J, Smith FD, Stark C, Wells CD, Fawcett JP, Kulkarni S, Metalnikov P, O'Donnell P, Taylor P, Taylor L, Zougman A, Woodgett JR, Langeberg LK, Scott JD, Pawson T (2004) Proteomic, functional, and domain-based analysis of in vivo 14-3-3 binding proteins involved in cytoskeletal regulation and cellular organization. *Curr Biol* 14(16):1436–1450. doi:[10.1016/j.cub.2004.07.051](https://doi.org/10.1016/j.cub.2004.07.051)
- Kaida A, Ariumi Y, Baba K, Matsubae M, Takao T, Shimotohno K (2005) Identification of a novel p300-specific-associating protein, PRS1 (phosphoribosylpyrophosphate synthetase subunit 1). *Biochem J* 391(Pt 2):239–247. doi:[10.1042/BJ20041308](https://doi.org/10.1042/BJ20041308)
- Khurana S, Chakraborty S, Cheng X, Su YT, Kao HY (2011) The actin-binding protein, actinin alpha 4 (ACTN4), is a nuclear receptor coactivator that promotes proliferation of MCF-7 breast cancer cells. *J Biol Chem* 286(3):1850–1859. doi:[10.1074/jbc.M110.162107](https://doi.org/10.1074/jbc.M110.162107)
- Kita K, Otsuki T, Ishizuka T, Ishijima S, Tatibana M (1989) Rat liver phosphoribosylpyrophosphate synthetase: existence as heterogeneous aggregates and identification of the catalytic subunit. *Adv Exp Med Biol* 253B:1–6. doi:[10.1007/978-1-4684-5676-9\\_1](https://doi.org/10.1007/978-1-4684-5676-9_1)
- Kita K, Ishizuka T, Ishijima S, Sonoda T, Tatibana M (1994) A novel 39-kDa phosphoribosylpyrophosphate synthetase-associated protein of rat liver. Cloning, high sequence similarity to the catalytic subunits, and a negative regulatory role. *J Biol Chem* 269(11):8334–8340
- Ko BS, Chang TC, Hsu C, Chen YC, Shen TL, Chen SC, Wang J, Wu KK, Jan YJ, Liou JY (2011) Overexpression of 14-3-3epsilon predicts tumour metastasis and poor survival in hepatocellular carcinoma. *Histopathology* 58(5):705–711. doi:[10.1111/j.1365-2559.2011.03789.x](https://doi.org/10.1111/j.1365-2559.2011.03789.x)
- Lee J, Mira-Arbibe L, Ulevitch RJ (2000) TAK1 regulates multiple protein kinase cascades activated by bacterial lipopolysaccharide. *J Leukoc Biol* 68(6):909–915
- Lodygin D, Hermeking H (2005) The role of epigenetic inactivation of 14-3-3sigma in human cancer. *Cell Res* 15(4):237–246. doi:[10.1038/sj.cr.7290292](https://doi.org/10.1038/sj.cr.7290292)
- Meek SE, Lane WS, Piwnica-Worms H (2004) Comprehensive proteomic analysis of interphase and mitotic 14-3-3-binding proteins. *J Biol Chem* 279(31):32046–32054. doi:[10.1074/jbc.M403044200](https://doi.org/10.1074/jbc.M403044200)
- Mendez-Sanchez N, Vasquez-Fernandez F, Zamora-Valdes D, Uribe M (2008) Sorafenib, a systemic therapy for hepatocellular carcinoma. *Ann Hepatol* 7(1):46–51. doi:[10.2147/BTT.S3410](https://doi.org/10.2147/BTT.S3410)
- Morrison DK (2009) The 14-3-3 proteins: integrators of diverse signaling cues that impact cell fate and cancer development. *Trends Cell Biol* 19(1):16–23. doi:[10.1016/j.tcb.2008.10.003](https://doi.org/10.1016/j.tcb.2008.10.003)
- Neal CL, Yao J, Yang W, Zhou X, Nguyen NT, Lu J, Danes CG, Guo H, Lan KH, Ensor J, Hittelman W, Hung MC, Yu D (2009) 14-3-3zeta overexpression defines high risk for breast cancer recurrence and promotes cancer cell survival. *Cancer Res* 69(8):3425–3432. doi:[10.1158/0008-5472.CAN-08-2765](https://doi.org/10.1158/0008-5472.CAN-08-2765)
- Niemantsverdriet M, Wagner K, Visser M, Backendorf C (2008) Cellular functions of 14-3-3 zeta in apoptosis and cell adhesion emphasize its oncogenic character. *Oncogene* 27(9):1315–1319. doi:[10.1038/sj.onc.1210742](https://doi.org/10.1038/sj.onc.1210742)
- Ninomiya-Tsujii J, Kishimoto K, Hiyama A, Inoue J, Cao Z, Matsumoto K (1999) The kinase TAK1 can activate the NIK-I kappaB as well as the MAP kinase cascade in the IL-1 signalling pathway. *Nature* 398(6724):252–256. doi:[10.1038/18465](https://doi.org/10.1038/18465)
- Nomura M, Shimizu S, Sugiyama T, Narita M, Ito T, Matsuda H, Tsujimoto Y (2003) 14-3-3 Interacts directly with and negatively regulates pro-apoptotic Bax. *J Biol Chem* 278(3):2058–2065. doi:[10.1074/jbc.M207880200](https://doi.org/10.1074/jbc.M207880200)
- Ong SE, Kratchmarova I, Mann M (2003) Properties of 13C-substituted arginine in stable isotope labeling by amino acids in cell culture (SILAC). *J Proteome Res* 2(2):173–181. doi:[10.1021/pr0255708](https://doi.org/10.1021/pr0255708)
- Parkin DM, Bray F, Ferlay J, Pisani P (2001) Estimating the world cancer burden: Globocan 2000. *Int J Cancer* 94(2):153–156. doi:[10.1002/ijc.1440](https://doi.org/10.1002/ijc.1440)
- Peng CY, Graves PR, Thoma RS, Wu Z, Shaw AS, Piwnica-Worms H (1997) Mitotic and G2 checkpoint control: regulation of 14-3-3 protein binding by phosphorylation of Cdc25C on serine-216. *Science* 277(5331):1501–1505. doi:[10.1126/science.2775331](https://doi.org/10.1126/science.2775331)
- Pereira-Faca SR, Kuick R, Puravs E, Zhang Q, Krasnoselsky AL, Phanstiel D, Qiu J, Misk DE, Hinderer R, Tammemagi M, Landi MT, Caporaso N, Pfeiffer R, Edelstein C, Goodman G, Barnett M, Thornquist M, Brenner D, Hanash SM (2007) Identification of 14-3-3 theta as an antigen that induces a humoral response in lung cancer. *Cancer Res* 67(24):12000–12006. doi:[10.1158/0008-5472.CAN-07-2913](https://doi.org/10.1158/0008-5472.CAN-07-2913)
- Pozuelo Rubio M, Geraghty KM, Wong BH, Wood NT, Campbell DG, Morrice N, Mackintosh C (2004) 14-3-3-affinity purification of over 200 human phosphoproteins reveals new links to regulation of cellular metabolism, proliferation and trafficking. *Biochem J* 379(Pt 2):395–408. doi:[10.1042/BJ20031797](https://doi.org/10.1042/BJ20031797)
- Premalatha B, Sujatha V, Sachdanandam P (1997) Modulating effect of *Semecarpus anacardium* Linn. nut extract on glucose metabolizing enzymes in aflatoxin B1-induced experimental hepatocellular carcinoma. *Pharmacol Res* 36(3):187–192. doi:[10.1006/phrs.1997.0214](https://doi.org/10.1006/phrs.1997.0214)
- Qi W, Liu X, Qiao D, Martinez JD (2005) Isoform-specific expression of 14-3-3 proteins in human lung cancer tissues. *Int J Cancer* 113(3):359–363. doi:[10.1002/ijc.20492](https://doi.org/10.1002/ijc.20492)
- Qi W, Liu X, Chen W, Li Q, Martinez JD (2007) Overexpression of 14-3-3gamma causes polyploidization in H322 lung cancer cells. *Mol Carcinog* 46(10):847–856. doi:[10.1002/mc.20314](https://doi.org/10.1002/mc.20314)
- Quaranta V (2002) Motility cues in the tumor microenvironment. *Differentiation* 70(9–10):590–598. doi:[10.1046/j.1432-0436.2002.700912.x](https://doi.org/10.1046/j.1432-0436.2002.700912.x)
- Sakurai H, Miyoshi H, Toriumi W, Sugita T (1999) Functional interactions of transforming growth factor beta-activated kinase 1 with IkappaB kinases to stimulate NF-kappaB activation.

- J Biol Chem 274(15):10641–10648. doi:[10.1074/jbc.274.15.10641](https://doi.org/10.1074/jbc.274.15.10641)
- Samuel T, Weber HO, Rauch P, Verdoodt B, Eppel JT, McShea A, Hermeking H, Funk JO (2001) The G2/M regulator 14-3-3sigma prevents apoptosis through sequestration of Bax. J Biol Chem 276(48):45201–45206. doi:[10.1074/jbc.M106427200](https://doi.org/10.1074/jbc.M106427200)
- Santoro MM, Gaudino G, Marchisio PC (2003) The MSP receptor regulates alpha6beta4 and alpha3beta1 integrins via 14-3-3 proteins in keratinocyte migration. Dev Cell 5(2):257–271. doi:[10.1016/S1534-5807\(03\)00201-6](https://doi.org/10.1016/S1534-5807(03)00201-6)
- Shaw RJ (2006) Glucose metabolism and cancer. Curr Opin Cell Biol 18(6):598–608. doi:[10.1016/j.ceb.2006.10.005](https://doi.org/10.1016/j.ceb.2006.10.005)
- Shevchenko A, Tomas H, Havlis J, Olsen JV, Mann M (2006) In-gel digestion for mass spectrometric characterization of proteins and proteomes. Nat Protoc 1(6):2856–2860. doi:[10.1038/nprot.2006.468](https://doi.org/10.1038/nprot.2006.468)
- Shibuya H, Yamaguchi K, Shirakabe K, Tonegawa A, Gotoh Y, Ueno N, Irie K, Nishida E, Matsumoto K (1996) TAB 1: an activator of the TAK1 MAPKKK in TGF-beta signal transduction. Science 272(5265):1179–1182. doi:[10.1126/science.2725265.1179](https://doi.org/10.1126/science.2725265.1179)
- Sivanesan D, Begum VH (2007) Modulatory effect of *Gynandropsis gynandra* L. on glucose metabolizing enzymes in aflatoxin B1-induced hepatocellular carcinoma in rats. Indian J Biochem Biophys 44(6):477–480
- Sonoda T, Ishizuka T, Kita K, Ishijima S, Tatibana M (1997) Cloning and sequencing of rat cDNA for the 41-kDa phosphoribosylpyrophosphate synthetase-associated protein has a high homology to the catalytic subunits and the 39-kDa associated protein. Biochim Biophys Acta 1350(1):6–10. doi:[10.1016/S0167-4781\(96\)00190-X](https://doi.org/10.1016/S0167-4781(96)00190-X)
- Tang S, Bai C, Yang P, Chen X (2013a) 14-3-3epsilon boosts bleomycin-induced DNA damage response by inhibiting the drug-resistant activity of MVP. J Proteome Res 12(6):2511–2524. doi:[10.1021/pr301085c](https://doi.org/10.1021/pr301085c)
- Tang S, Bao H, Zhang Y, Yao J, Yang P, Chen X (2013b) 14-3-3epsilon mediates the cell fate decision-making pathways in response of hepatocellular carcinoma to Bleomycin-induced DNA damage. PLoS One 8(3):e55268. doi:[10.1371/journal.pone.0055268](https://doi.org/10.1371/journal.pone.0055268)
- Tatibana M, Kita K, Taira M, Ishijima S, Sonoda T, Ishizuka T, Iizasa T, Ahmad I (1995) Mammalian phosphoribosyl-pyrophosphate synthetase. Adv Enzyme Regul 35:229–249. doi:[10.1016/0065-2571\(94\)00017-W](https://doi.org/10.1016/0065-2571(94)00017-W)
- Thomas MB, Abbruzzese JL (2005) Opportunities for targeted therapies in hepatocellular carcinoma. J Clin Oncol 23(31):8093–8108. doi:[10.1200/JCO.2004.00.1537](https://doi.org/10.1200/JCO.2004.00.1537)
- Thomas D, Guthridge M, Woodcock J, Lopez A (2005) 14-3-3 protein signaling in development and growth factor responses. Curr Top Dev Biol 67:285–303. doi:[10.1016/S0070-2153\(05\)67009-3](https://doi.org/10.1016/S0070-2153(05)67009-3)
- Trinkle-Mulcahy L, Boulon S, Lam YW, Urcia R, Boisvert FM, Vandermoere F, Morrice NA, Swift S, Rothbauer U, Leonhardt H, Lamond A (2008) Identifying specific protein interaction partners using quantitative mass spectrometry and bead proteomes. J Cell Biol 183(2):223–239. doi:[10.1083/jcb.200805092](https://doi.org/10.1083/jcb.200805092)
- Tzivion G, Gupta VS, Kaplun L, Balan V (2006) 14-3-3 proteins as potential oncogenes. Semin Cancer Biol 16(3):203–213. doi:[10.1016/j.semcancer.2006.03.004](https://doi.org/10.1016/j.semcancer.2006.03.004)
- van Hemert MJ, Steensma HY, van Heusden GP (2001) 14-3-3 proteins: key regulators of cell division, signalling and apoptosis. Bioessays 23(10):936–946. doi:[10.1002/bies.1134](https://doi.org/10.1002/bies.1134)
- van Heusden GP (2005) 14-3-3 proteins: regulators of numerous eukaryotic proteins. IUBMB Life 57(9):623–629. doi:[10.1080/15216540500252666](https://doi.org/10.1080/15216540500252666)
- Wang T, Gu S, Ronni T, Du YC, Chen X (2005) In vivo dual-tagging proteomic approach in studying signaling pathways in immune response. J Proteome Res 4(3):941–949. doi:[10.1021/pr050031z](https://doi.org/10.1021/pr050031z)
- Wilker E, Yaffe MB (2004) 14-3-3 proteins—a focus on cancer and human disease. J Mol Cell Cardiol 37(3):633–642. doi:[10.1016/j.yjmcc.2004.04.015](https://doi.org/10.1016/j.yjmcc.2004.04.015)
- Yamaguchi K, Shirakabe K, Shibuya H, Irie K, Oishi I, Ueno N, Taniguchi T, Nishida E, Matsumoto K (1995) Identification of a member of the MAPKKK family as a potential mediator of TGF-beta signal transduction. Science 270(5244):2008–2011. doi:[10.1126/science.2705244.2008](https://doi.org/10.1126/science.2705244.2008)
- Yang X, Zou P, Yao J, Yun D, Bao H, Du R, Long J, Chen X (2010) Proteomic dissection of cell type-specific H2AX-interacting protein complex associated with hepatocellular carcinoma. J Proteome Res 9(3):1402–1415. doi:[10.1021/pr900932y](https://doi.org/10.1021/pr900932y)
- Yao M, Zhou XD, Zha XL, Shi DR, Fu J, He JY, Lu HF, Tang ZY (1997) Expression of the integrin alpha5 subunit and its mediated cell adhesion in hepatocellular carcinoma. J Cancer Res Clin Oncol 123(8):435–440. doi:[10.1007/BF01372547](https://doi.org/10.1007/BF01372547)
- Zha J, Harada H, Yang E, Jockel J, Korsmeyer SJ (1996) Serine phosphorylation of death agonist BAD in response to survival factor results in binding to 14-3-3 not BCL-X(L). Cell 87(4):619–628. doi:[10.1016/S0092-8674\(00\)81382-3](https://doi.org/10.1016/S0092-8674(00)81382-3)
- Zuo S, Xue Y, Tang S, Yao J, Du R, Yang P, Chen X (2010) 14-3-3 epsilon dynamically interacts with key components of mitogen-activated protein kinase signal module for selective modulation of the TNF-alpha-induced time course-dependent NF-kappaB activity. J Proteome Res 9(7):3465–3478. doi:[10.1021/pr9011377](https://doi.org/10.1021/pr9011377)